ACS OMEGA

http://pubs.acs.org/journal/acsodf

Article

Valerenic Acid Promotes Adipocyte Differentiation, Adiponectin Production, and Glucose Uptake *via* Its PPARγ Ligand Activity

Jun Takahashi, Nobuyuki Takahashi, Miki Tadaishi, Makoto Shimizu, and Kazuo Kobayashi-Hattori*

Cite This: *ACS Omega* 2022, 7, 48113−48120

Read Online

ACCESS | Metrics & More | Article Recommendations | Supporting Information

ABSTRACT: Although valerenic acid (VA) is an important marker compound for quantitative assessment of *Valeriana officinalis* products, little is known about its potential effects on adipocytes. We investigated the effects of VA on adipocyte differentiation, adiponectin production, and glucose uptake using 3T3-L1 adipocytes. The results showed that VA promoted adipocyte differentiation and increased the gene expression of adipogenesis and glucose uptake-related proteins, including peroxisome proliferator-activated receptor gamma (PPARγ), cytosine-cytosine-adenosine-adenosine-thymidine enhancer binding protein alpha (C/EBPα), adiponectin, and glucose transporter 4 (GLUT4). Additionally, cell cultures treated with VA had elevated adiponectin secretion and glucose uptake. The PPARγ luciferase assay indicated VA as a partial agonist of PPARγ, while the analysis using its antagonist, GW9662, and a docking simulation between PPARγ and VA revealed the binding site of VA as likely adjacent to the Ω loop pocket of PPARγ. Taken together, these results demonstrate that VA acts as a PPARγ partial agonist to promote adipocyte differentiation, adiponectin production, and glucose uptake.

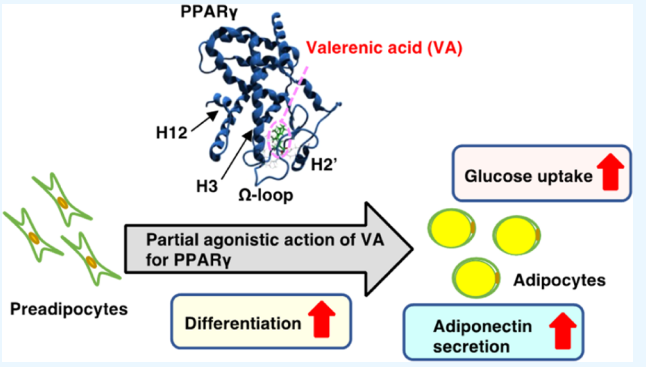

1. INTRODUCTION

Diabetes mellitus is a metabolic disorder caused by lack of insulin activity.[1,2] In particular, type 2 diabetes is characteristically linked to lifestyle abnormity and obesity. Diabetes prevalence among adults was estimated to be 8.8% in 2015, and it is predicted to rise to 10.4% in 2040.[3] The development of diabetes induces related complications such as nephropathy, blindness, and cardiomyopathy.[4,5] A systematic review also identified a strong association between type 2 diabetes and non-alcoholic fatty liver disease (NAFLD).[6] In addition, patients with diabetes have a higher prevalence of steatohepatitis, liver fibrosis, and end-stage liver disease.[7] NAFLD is also significantly associated with a 2-fold increased risk of incident diabetes.[8] Therefore, it is important to prevent diabetes and NAFLD at an early stage. The basic treatment for these diseases is weight loss (especially visceral fat), achieved by diet and exercise. For example, a lifestyle-modification program with the goals of at least a 7% weight loss and at least 150 min of physical activity per week reduced the incidence of type 2 diabetes by 58%.[9] An intensive lifestyle intervention also reduced the risk of diabetes by an average of 16% per kilogram of weight loss.[10] The treatment of NAFLD should be also directed at reducing visceral adipose tissue stores during the earliest stages of disease development.[11] Therefore, reducing body weight (abdominal fat) is the clinically correct approach to the treatment of diabetes.

In contrast, much of the basic research into anti-diabetic activity has focused on adipocytes, which are a component of adipose tissue, because numerous studies examining the predisposing factors of diabetes have revealed that adipose tissues are closely associated with disease development.[12] Adipocytes are involved in the energy storage and maintenance of energy homeostasis *via* adipokine secretion.[13] Adiponectin is an adipokine with positive effects on diabetes and can activate AMP-activated protein kinase (AMPK) and peroxisome proliferator-activated receptor α (PPARα), subsequently promoting glucose uptake and fatty acid oxidation.[14] However, adiponectin secretion is down-regulated by hypertrophy of adipocytes.[15] The adipocyte size is correlated with insulin sensitivity, with its increase in size causing a decrease in sensitivity.[16] In addition, hypertrophied adipocytes secrete numerous mediators, such as free fatty acid, tumor necrosis factor-α, and monocyte chemoattractant protein-1 that cause chronic inflammation. These mediators can lead to insulin resistance[17] and impaired biological response to insulin stimulation in target tissues, including liver, muscle, and adipose tissue. This suggests that increasing adiponectin secretion and miniaturizing adipocytes could potentially

Received: September 22, 2022
Accepted: November 28, 2022
Published: December 13, 2022

attenuate insulin resistance to produce beneficial effects against type 2 diabetes.

Various food components and plant extracts with similar beneficial effects have been reported. For example, 3T3-L1 cells were used to demonstrate that fenugreek could improve glucose metabolism by promoting adipocyte differentiation and inhibiting inflammation in the adipose tissues of type 2 diabetic mice, and diosgenin was identified as the active compound in fenugreek extract.[18] Apo-12′-lycopenal, which is a lycopene-derived metabolite, promoted adipocyte differentiation and adiponectin secretion through PPARγ activation in 3T3-L1 adipocytes.[19] Similarly, we previously showed that hot water extracts of edible *Chrysanthemum morifolium* could induce adipocyte differentiation and adiponectin secretion in 3T3-L1 cells,[20] leading to decreased blood glucose level and improved insulin resistance in KK-A^{y} mice.[21] Recently, we have demonstrated that methanolic *Valeriana officinalis* root extract could promote adipocyte differentiation and adiponectin production in 3T3-L1 adipocytes and identified valerenic acid (VA) as one of the likely active components.[22] Although VA has been reported to have anxiolytic activity[23] and central nervous depressant activity,[24] its potential effects on adipocytes are yet to be determined.

Thus, our study aimed to investigate the likely capacity of VA in promoting adipocyte differentiation, adiponectin production, and glucose uptake using 3T3-L1 cells. In addition, antagonist and docking simulation assays were conducted to determine the binding mode of VA to PPARγ. Our results suggest that VA acts as a PPARγ partial agonist to promote adipocyte differentiation, adiponectin production, and glucose uptake and provide a new insight on the action of VA as a partial PPARγ agonist.

2. RESULTS AND DISCUSSION

The possible effects of VA on the differentiation of 3T3-L1 adipocytes were initially examined (Figure 1). As a result, remarkable adipocyte differentiation was observed with 100 μM VA but not with treatment at 1 and 10 μM concentrations (Figure 1a). In addition, TG accumulation at 100 μM VA was significantly higher than that of the control (Figure 1b). These results showed that VA induced 3T3-L1 adipocyte differentiation.

Subsequently, the effects of VA on the expression of adipogenesis-related genes were investigated (Figure 2). PPARγ, a master regulator of adipocytes differentiation, and CCAAT/enhancer binding protein α (C/EBPα), mutually regulate each other and are associated with the expression of adipocyte phenotypes.[25] Compared to the control, no detectable change in mRNA levels of PPARγ and C/EBPα were observed with 1 and 10 μM VA treatments, while VA at 100 μM significantly increased their mRNA levels (Figure 2a,b). In addition, 100 μM VA significantly enhanced the mRNA levels of adipocyte protein 2 (aP2) and lipoprotein lipase (LPL), which are both regulated by PPARγ (Figure 2c,d). Together, these results suggested that VA could induce adipocyte differentiation through up-regulation of PPARγ.

Adiponectin, which is also targeted by PPARγ, can act on the liver and skeletal muscle to promote fatty acid oxidation and glucose uptake in the absence of insulin.[16] Interestingly, adiponectin levels have been reported to be lower in individuals at risk of type 2 diabetes mellitus than in healthy individuals.[26] Therefore, up-regulation of adiponectin can contribute to amelioration of glucose metabolism. Relative to

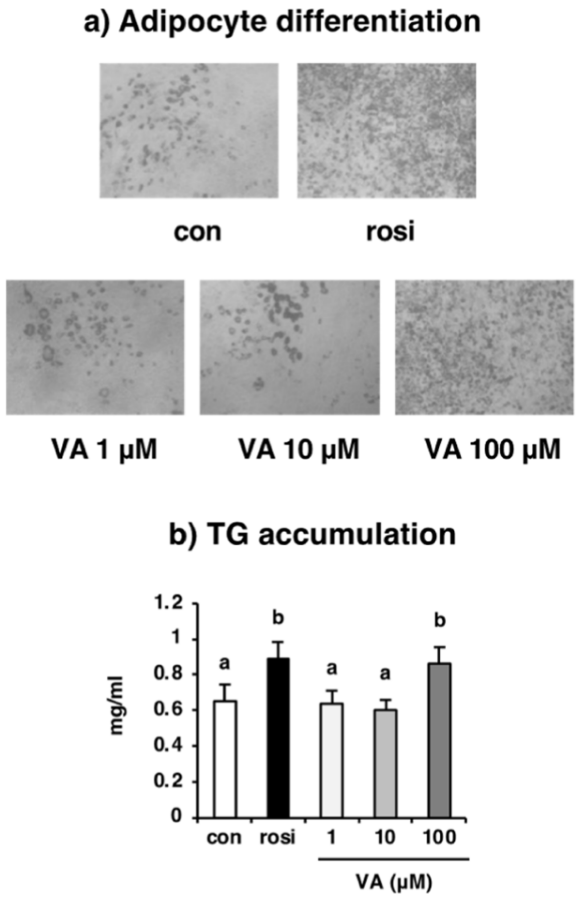

Figure 1. Effects of VA on the differentiation of 3T3-L1 adipocytes. (a) Lipid droplets in 3T3-L1 cells as visualized by Oil red O staining. Rosiglitazone (Rosi), a PPARγ agonist, was used as a positive control. (b) TG accumulation in 3T3-L1 cells as measured using the TG E-test Wako kit. Data are expressed as mean ± SD (n = 4). Data with different letters represent significant differences at $p < 0.05$.

control groups, treatment with 1 or 10 μM VA showed no effect on the mRNA and protein levels of adiponectin (Figure 3a,b), whereas their levels were significantly increased with 100 μM VA. These results suggested that VA could potentially improve glucose metabolism through adiponectin induced by up-regulation of PPARγ.

The glucose uptake assay in the presence of insulin using 2-NBDG, which is a fluorescent glucose analogue, showed that glucose uptake was significantly increased with 100 μM VA but not with 1 and 10 μM VA concentrations (Figure 4a). In addition, the mRNA level of glucose transporter 4 (GLUT4), which is regulated by PPARγ, was significantly increased with 100 μM VA (Figure 4b). Therefore, it is likely that VA could enhance GLUT4 expression by up-regulating PPARγ and thereby promote glucose uptake in the presence of insulin.

The above results demonstrated the interaction between VA and PPARγ in regulating adipocyte differentiation, adiponectin production, and glucose uptake; however, the mechanism of VA activity on PPARγ is still unclear. Consequently, the potential role of VA as a ligand-dependent activator of PPARγ transcriptional activity was examined (Figure 5). As shown in Figure 5a, 10 μM VA could not induce PPARγ activation, but its transcriptional activity was significantly enhanced with 100 μM VA. In addition, the mRNA level of aP2, which is a mature adipocyte marker and a target gene of PPARγ, was measured

https://doi.org/10.1021/acsomega.2c06120
ACS Omega 2022, 7, 48113−48120

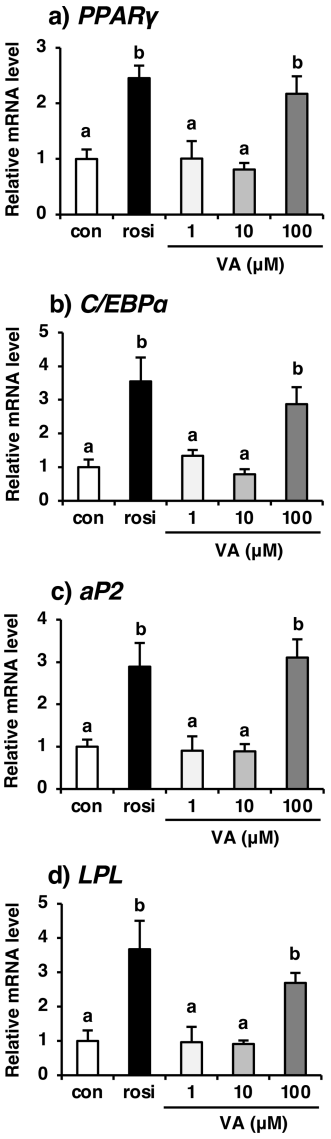

Figure 2. Effect of VA on the mRNA level of transcription factors related to adipocyte differentiation in 3T3-L1 adipocytes. The mRNA levels of (a) PPARγ, (b) C/EBPα, (C) aP2, and (D) LPL in 3T3-L1 adipocytes as measured with qPCR. The mRNA levels of target genes are expressed as values relative to those of β-actin. Data are expressed as mean ± SD (n = 4). Data with different letters represent significant differences at $p < 0.05$.

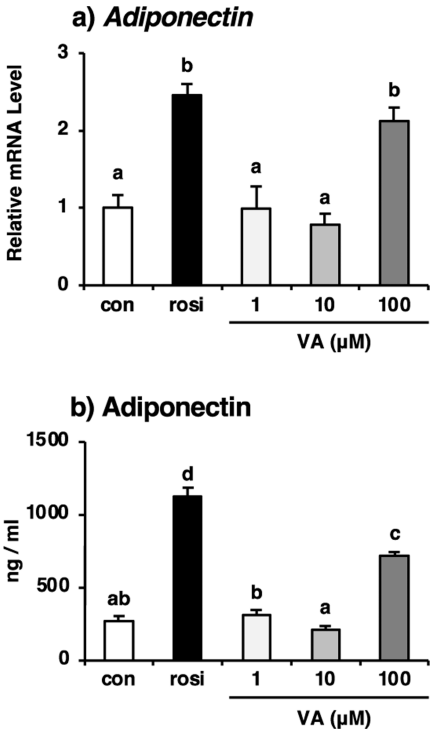

Figure 3. Effect of VA on adiponectin secretion in 3T3-L1 adipocytes. (a) The mRNA level of adiponectin in 3T3-L1 adipocytes were measured by qPCR, and the levels were expressed as values relative to that of β-actin. (b) Adiponectin level in the cell culture supernatant as determined by the mouse/rat adiponectin ELISA kit. Data are expressed as mean ± SD (n = 4). Data with different letters represent significant differences at $p < 0.05$.

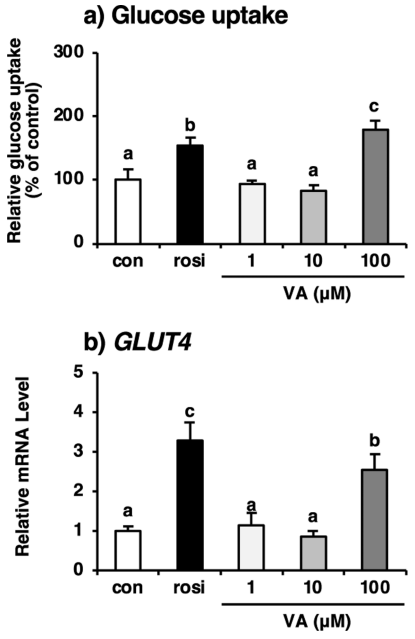

Figure 4. Effect of VA on glucose uptake in 3T3-L1 adipocytes. (a) Glucose uptake in 3T3-L1 cells as measured with 2-NBDG. (b) mRNA levels of GLUT4 as determined by qPCR and expressed as values relative to that of β-actin. Data are expressed as mean ± SD (n = 6). Data with different letters represent significant differences at $p < 0.05$.

after addition of VA and rosi from the seventh to eighth day of 3T3-L1 cell culture (Figure 5b). As a result, addition of 100 μM VA significantly increased the mRNA level of aP2. PPARγ expression is usually transcriptionally activated two days after induction of differentiation, and peaks by the third or fourth day.[27] Therefore, since PPARγ seems to have been sufficiently induced between the seventh to eighth day in our study, the results of ap2 expression after adding VA during the same period support that VA is a PPARγ ligand rather than an inducer of PPARγ expression. Notably, the transcriptional activation capacity of VA for PPARγ at 100 μM was significantly weaker than that of 1 μM pioglitazone (pio; a PPARγ full agonist) (Figure 5a), suggesting that VA is a partial PPARγ agonist.

PPARγ has two large ligand-binding pockets (LBPs) of approximately 1300−1440 Å[28] and can bind to various types of

https://doi.org/10.1021/acsomega.2c06120
ACS Omega 2022, 7, 48113−48120

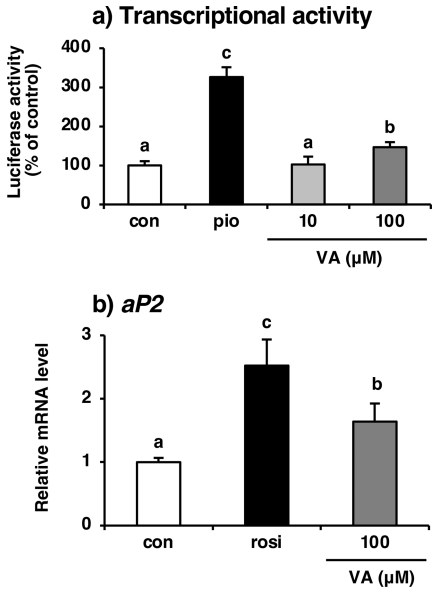

Figure 5. Effect of VA on PPARγ transcriptional activity. (a) PPARγ transcriptional activity as measured with luciferase assay using 10T1/2 cells. The final concentrations of VA and pioglitazone (pio) used were 10 or 100 μM and 1 μM, respectively. (b) Confirmation that VA is a PPARγ ligand. VA and rosi were added on the seventh to eighth day after inducing the differentiation of 3T3-L1 cells, followed by measurement of aP2 mRNA levels. Data are expressed as mean ± SD ($n = 6$). Data with different letters represent significant differences at $p < 0.05$.

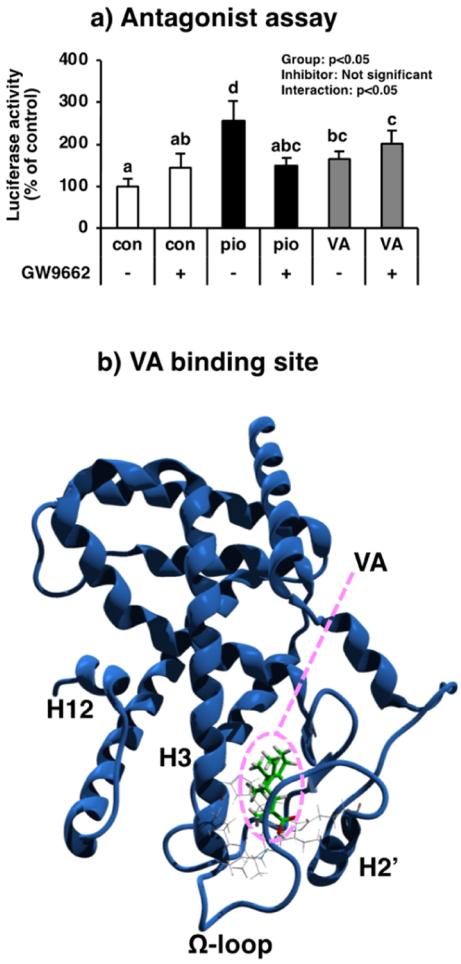

Figure 6. Analysis of possible VA binding sites on PPARγ. (a) Antagonist assay using GW9662. To predict the binding mode of VA to PPARγ, PPARγ transcriptional activation was measured with luciferase assay in 10T1/2 cells treated with 100 and 1 μM for VA and pio, respectively, and with or without 10 μM GW9662. Data are expressed as mean ± SD (n = 5−6). Data with different letters represent significant differences at $p < 0.05$. (b) Putative binding mode of VA (green) to PPARγ LBD and a summary image of the VA/PPARγ LBD complex.

ligands.[29,30] PPARγ LBPs are Y-shaped, and each sub-pocket is known as activation function-2 (AF2) (the canonical LBP) pocket adjacent to Helix (H) 12 and the Ω loop pocket located near H2'. Thiazolidinediones (TZDs) are active PPARγ full agonists, which bind to His 323, His 449, and Tyr 473 on the AF2 surface *via* a hydrogen bond, resulting in the stabilization of the AF2 region in PPARγ.[31,32] The stabilization of the AF2 region facilitates the association of co-activators containing LXXLL motif, such as steroid receptor co-activating factor and PPARγ co-activator-1α, thereby activating the transcriptional activity of PPARγ.[28,32] However, the transcriptional activation of PPARγ is inhibited by covalent antagonists, such as GW9662 and T0070907,[33] due to the close proximity of their binding sites to Cys285 in H3. In contrast, since partial agonists, including indomethacin and 5-methoxy-indole acetate, can bind near AF2 and the Ω loop without Cys285, their transcriptional activation of PPARγ is not blocked by these covalent antagonists.[34] In addition, luteolin, which acts near the Ω loop, could inhibit adipogenesis[35] but enhance PPARγ transcriptional activation in the presence of GW9662.[36] Therefore, an antagonist assay with GW9662 was performed to determine the binding mode of VA (Figure 6a). A two-way ANOVA test revealed a significant interaction between group and inhibitor ($p < 0.05$). Subsequent multiple comparison tests showed that pio and VA significantly increased PPARγ transcriptional activity in the absence of GW9662. Notably, addition of GW9662 significantly inhibited the pio-induced transcriptional activation of PPARγ, but no change in VA-induced transcriptional activation was observed. These results suggest that VA acts adjacent to the AF2 or Ω loop pockets rather than *via* the Cys-mediated binding mode of H3, which is the site of GW9662 activity. Furthermore, we analyzed the binding mode of VA using docking simulations. Our results suggest that VA might bind adjacent to the Ω loop pocket and form hydrogen bonds with Glu 259 of H2′, Ile 267 of Ω loop, and Arg 280 of H3 in PPARγ (Figures 6b; S1). The docking simulation also showed that VA had steric interactions with Leu 255 and Glu 259 of H2′ and His 266 of Ω loop in PPARγ (Figure S2). Interestingly, partial agonists that bind close to the Ω loop, which is not a full agonist binding site, have been also reported to have anti-diabetic activity. For example, MRL24 that binds near the Ω loop pocket ameliorated high-fat diet (HFD)-induced diabetes.[37] A synthetic ligand S35 that binds hydrogen to Leu270 and Gln 283 in the Ω loop pocket inhibited the phosphorylation of Ser245 in PPARγ by the cyclin-dependent kinase 5,[38] and the resulting effect is associated with diabetic profiles.[32] Therefore, it is likely that VA harbors similar positive effect on diabetes as a partial agonist by inducing the binding of PPARγ to the Ω loop pocket.

Our study is the first to show that VA affects adipocyte function *via* a PPARγ partial agonist activity *in vitro*. However, the concentration (100 μM) used in this study appears to be

https://doi.org/10.1021/acsomega.2c06120
ACS Omega 2022, 7, 48113−48120

high because the average peak serum concentrations of VA after single or multiple doses (300 mg/dose) of *V. officinalis* root extract in older women were both approximately 3.3 ng/mL (0.014 μM).[39] In this study, the extract contained approximately 0.5% VA; that is, 300 mg of the extract would contain 1.5 mg of VA. Thus, it is estimated that the ingestion of 1.5 mg of VA resulted in a blood VA concentration of 3.3 ng/mL. Based on this value, to achieve a blood VA concentration of 100 μM (23.43 μg/mL), 10,650 mg of VA would need to be ingested [{1.5 × (23.43 × 1000/3.3)} = 10,650 mg]. As the average weight of the older women participating in the study of Anderson *et al.*[39] was 70 kg, the expected dose was 152 mg/kg (10650 mg/70 kg = 152 mg/kg). Compared with the doses of VA used in *in vivo* studies, this is a relatively high expected dose. For example, mice orally administered 0.5 mg/kg of valerian extract with a high VA and low AVA content (12:1) exhibited significant anxiolytic activity.[40] Mice intraperitoneally injected with 50 and 100 mg/kg VA had significantly prolonged pentobarbital-induced sleeping time.[24] Therefore, the dose (152 mg/kg) expected to be necessary to reach a blood concentration of 100 μM is likely not only to affect adipocyte function but also to exert anxiolytic and central nervous system depressant activities. Additionally, VA may affect hepatocytes as well. The study by Pan *et al.* suggested that the upregulation of adipocyte-specific genes in the liver, such as aP2 and PPARγ, was related to hepatocytic lipid accumulation and was involved in the development of hepatic steatosis.[41] As VA increased the mRNA expression of aP2 and PPARγ in adipocytes (Figure 2), it is possible that VA may contribute to the development of hepatic steatosis. Although there are some reports on the effect of VA on hepatocytes,[42−44] no information is available on the effect of VA on hepatic steatosis. Future *in vivo* experiments using animal models are needed to examine the actions of VA for potential medical applications.

3. CONCLUSIONS

In our previous study, we found that *V. officinalis* methanolic root extract could promote adipocyte differentiation and adiponectin production in 3T3-L1 adipocytes and identified VA as one of the likely active components.[22] However, the detailed effects of VA on adipocytes and its mechanism were not identified. The results of the present study showed that VA promoted adipocyte differentiation, adiponectin secretion, and glucose uptake. These effects resulted from the partial agonist ability of VA on PPARγ. In addition, the antagonist assay using GW9662 and the docking simulation between PPARγ and VA revealed that the binding site of VA was adjacent to the Ω loop pocket of PPARγ. These findings on the binding mode between VA and PPARγ provide new insights into the action of VA as a PPARγ partial agonist.

4. MATERIALS AND METHODS

4.1. Cell Culture. The 3T3-L1 cells were obtained from the Japanese Collection of Research Bioresourses (JCRB, Osaka, Japan). Cells at a concentration of 5.0 × 10^3 cells/mL in 24-well plates were cultured at 37 °C in a humidified atmosphere of 5% CO_2, with a pre-adipocyte maintenance medium containing Dulbecco's modified Eagle's medium, DMEM (4.5 g/L glucose) (FUJIFILM Wako Pure Chemical Corporation, Osaka, Japan) supplemented with 10% bovine serum (Thermo Fisher Scientific Inc., Waltham, MA) and 1% penicillin−streptomycin (Thermo Fisher Scientific Inc). Two days post-confluence formation, the medium was replaced with an adipocyte differentiation medium and cultured separately with or without VA (Extrasynthese S.A., Genay, France) for 8 days as previously described.[22] Rosiglitazone (rosi) (FUJIFILM Wako Pure Chemical Corporation) at a final concentration of 100 nM was added to the adipocyte differentiation medium during the first 2 days as a positive control. Dimethyl sulfoxide (DMSO) was used as a vehicle at a final concentration of 0.1% (v/v).

4.2. Oil Red O Staining Assay. Oil red O staining was performed as previously described.[22] Briefly, differentiated cells on the eighth day were washed with phosphate-buffered saline (PBS) before fixing with 10% formalin for 1 h. Cells were subsequently washed twice with 60% isopropanol and incubated with Oil red O solution (Sigma-Aldrich Co. LLC., St. Louis, MO) for 20 min. After rinsing and adding pure water to the wells, photographs were taken with a μv5300Peltier camera (Matsusada Precision, Inc., Shiga, Japan) mounted on a microscope.

4.3. TG Quantification Assay. The cellular concentration of triglyceride (TG) was determined using the method of Senarath *et al.*[45] with a few modifications. Briefly, mature adipocytes obtained on the eighth day were rinsed twice with PBS; the cells were scraped into PIPES (Piperazine-*N*,*N*′-*bis*(2-ethanesulfonic acid)) buffer with 0.1% Triton X and lysed by sonication on ice. The TG level in the lysate was measured using the triglyceride E-test Wako kit (FUJIFILM Wako Pure Chemical Corporation) according to the manufacture's protocol.

4.4. RNA Extraction and qPCR. Total RNA was isolated from 3T3-L1 cells (8.0 × 10^3 cells/mL) on the eighth day of culture in a 6-well plate using ISOGENII reagent (Nippon Gene Co., Ltd., Tokyo, Japan) according to the manufacturer's instructions. cDNA was synthesized using PrimeScript RT reagent kit with gDNA Eraser (perfect real-time) (Takara Bio Inc., Shiga, Japan) according to the manufacturer's instructions. qPCR was performed on an ABI PRISM 7300 Sequence Detection System (Thermo Fisher Scientific Inc.) using THUNDERBIRD SYBR Green and primer sets (Table 1). The PCR program was set as follows: initial denaturation at 95 °C for 1 min, followed by 40 cycles at 95 °C for 15 s and 60 °C for 1 min.

Table 1. Sequence of the Primers Used for qPCR

Genes		sequences (5′ to 3′)
β-actin	forward	AACGAGCGGTTCCGATGC
	reverse	GTGTTGGCATAGAGGTCTTTACGG
PPARγ	forward	GCTTGTGAAGGATGCAAGGGTT
	reverse	GCATCCGCCCAAACCTGATG
C/EBPα	forward	AGTCGGTGGACAAGAACAGC
	reverse	ACTGGTCAACTCCAGCACCTTC
Adiponectin	forward	ACTTGTGCAGGTTGGATGGC
	reverse	GCCCTTCAGCTCCTGTCATTC
aP2	forward	TTCCTTCAAACTGGGCGTGG
	reverse	CCATCCCACTTCTGCACCTG
LPL	forward	GCAACATTGGAGAAGCCATCCG
	reverse	GTTGCACCTGTATGCCTTGCTG
GLUT4	forward	TTGGACGGTTCCTCATTGGC
	reverse	GGTTGAGTGTTCCCAAGGCA

https://doi.org/10.1021/acsomega.2c06120
ACS Omega 2022, 7, 48113−48120

4.5. Adiponectin Quantification Assay. Adiponectin levels in culture supernatants obtained on the eighth day were quantified with the mouse/rat adiponectin ELISA kit (Otsuka Pharmaceutical Co., Ltd., Tokyo, Japan) according to the manufacture's protocol.

4.6. Glucose Uptake Assay. Glucose uptake assay was performed following the method described by Manaharan *et al.*[46] Briefly, the 3T3-L1 pre-adipocytes at a concentration of 4.0×10^3 cells/mL in the pre-adipocyte maintenance medium were seeded at 200 μL/well in 96-well black plates and then cultured until 2 days post-confluence formation. The cells were cultured separately in the adipocyte differentiation medium with or without VA for 8 days as aforementioned. After washing twice with PBS, the cells were cultured for 3 h in a serum-free DMEM containing 80 mM 2-[*N*-(7-nitrobenz-2-oxa-1,3-diazol-4-yl)amino]-2-deoxy-D-glucose (2-NBDG) and 100 nM insulin. Intracellular fluorescence intensities of 2-NBDG were detected with a microplate reader (PowerscanHT, BioTek Instruments, Inc., Winooski, VT).

4.7. Luciferase Reporter Assay. The PPARγ ligand assay was performed with a human GAL4/PPARγ ligand-binding domain chimera system using a 10T1/2 mesenchymal stem cell line as previously described.[47] Briefly, 10T1/2 cells at a concentration of 5.0×10^3 cells/mL were cultured in a 6-well plate with 10% FBS medium [DMEM containing 10% FBS (Sigma-Aldrich Co. LLC.) and 1% penicillin−streptomycin] until a 60% confluence was achieved. For transfection, the cells were incubated for 5 h in 300 μL Opti-MEM (Thermo Fisher Scientific Inc.) containing 1 μg GAL4/PPARγ ligand-binding domains (LBD) vector, 1 μg UAS-tk-luciferase reporter vector (the information of these vectors were previously described[48]), and 15 μL lipofectamine (Thermo Fisher Scientific Inc). After incubation, cells were transferred to a 96-well plate containing 10% FBS medium with assay compounds, including pioglitazone (as a PPARγ agonist), GW9662 (as PPARγ antagonist), and VA at final concentrations of 1, 10, and 10 or 100 μM, respectively. DMSO at a final concentration of 0.1% (v/v) was used as the only vehicle control. After 24 h incubation, transfected cells were used for luciferase assay according to the manufacturer's procedure (Promega, Madison, WI). The chemiluminescence was measured with the PowerscanHT microplate reader (BioTek Instruments, Inc).

4.8. Molecular Docking Assay. Molecular docking study of VA for human PPARγ LBD was performed with Molegro virtual Docker ver. 7.0.1 (Molexus IVS, Odder, Denmark). Protein structures of the human PPARγ LBD and VA were retrieved from Protein Data Bank and PubChem with the PDB code and PubChem CID of 1PRG and 6440940, respectively, then imported into the docking program according to the software instructions. The potential ligand-binding sites of protein or the volume of the open cavity was calculated using the Molegro cavity detection algorithm. Docking simulations were performed with their default procedures. The docking algorithm used in this study to search docked poses was based on an evolutionary MolDock Optimizer algorithm. After obtaining multiple poses, clustering algorithm using root mean square deviation was performed to exclude similar poses. To reduce contingency of docking results, their docking programs were analyzed with over 10 iterations.

4.9. Statistical Analysis. Statistical analysis was performed using SPSS software ver. 21. The data were presented as mean ± standard deviation (SD). The means of different groups were compared using one-way ANOVA or two-way ANOVA followed by Tukey multiple range test.

■ ASSOCIATED CONTENT

Supporting Information

The Supporting Information is available free of charge at https://pubs.acs.org/doi/10.1021/acsomega.2c06120.

Magnified view of binding between VA and amino acids of PPARγ and amino acids of PPARγ related to binding to VA (PDF)

■ AUTHOR INFORMATION

Corresponding Author

Kazuo Kobayashi-Hattori − *Department of Nutritional Science, Faculty of Applied Bioscience, Tokyo University of Agriculture, Tokyo 156-8502, Japan;* orcid.org/0000-0002-0921-2128; Phone: +81-3-5477-2443; Email: k2kobaya@nodai.ac.jp

Authors

Jun Takahashi − *Department of Nutritional Science, Faculty of Applied Bioscience, Tokyo University of Agriculture, Tokyo 156-8502, Japan;* Present Address: R&D Division, Hayashibara Co., Ltd., 675-1 Fujisaki, Naka-ku, Okayama 702-8006, Japan

Nobuyuki Takahashi − *Department of Nutritional Science and Food Safety, Faculty of Applied Bioscience, Tokyo University of Agriculture, Tokyo 156-8502, Japan*

Miki Tadaishi − *Department of Nutritional Science, Faculty of Applied Bioscience, Tokyo University of Agriculture, Tokyo 156-8502, Japan*

Makoto Shimizu − *Department of Nutritional Science, Faculty of Applied Bioscience, Tokyo University of Agriculture, Tokyo 156-8502, Japan*

Complete contact information is available at: https://pubs.acs.org/10.1021/acsomega.2c06120

Notes

The authors declare no competing financial interest.

■ REFERENCES

(1) Schmidt, A. M. Highlighting diabetes—the epidemic continues. *Arterioscler. Thromb. Vasc. Biol.* **2018**, *38*, e1−e8.

(2) Khin, P.-P.; Lee, J.-H.; Jun, H.-S. A brief review of the mechanisms of β-Cell dedifferentiation in type 2 diabetes. *Nutrients* **2021**, *13*, 1593.

(3) Ogurtsova, K.; da Rocha Fernandes, J. D.; Huang, Y.; Linnenkamp, U.; Guariguata, L.; Cho, N. H.; Cavan, D.; Shaw, J. E.; Makaroff, L. E. IDF Diabetes Atlas: Global estimates for the prevalence of diabetes for 2015 and 2040. *Diabetes Res. Clin. Pract.* **2017**, *128*, 40−50.

(4) Tziomalos, K.; Athyros, V. G. Diabetic nephropathy: New risk factors and improvements in diagnosis. *Rev. Diabet. Stud.* **2015**, *12*, 110−118.

(5) Katakami, N. Mechanism of development of atherosclerosis and cardiovascular disease in diabetes mellitus. *J. Atheroscler. Thromb.* **2018**, *25*, 27−39.

(6) Vernon, G.; Baranova, A.; Younossi, Z. M. Systematic review: the epidemiology and natural history of non-alcoholic fatty liver disease and non-alcoholic steatohepatitis in adults. *Aliment. Pharmacol. Ther.* **2011**, *34*, 274−285.

(7) Gastaldelli, A.; Cusi, K. From NASH to diabetes and from diabetes to NASH: Mechanisms and treatment options. *JHEP Rep* **2019**, *1*, 312−328.

(8) Mantovani, A.; Byrne, C. D.; Bonora, E.; Targher, G. Nonalcoholic fatty liver disease and risk of incident type 2 diabetes: A meta-analysis. *Diabetes Care* **2018**, *41*, 372−382.
(9) Knowler, W. C.; Barrett-Connor, E.; Fowler, S. E.; Hamman, R. F.; Lachin, J. M.; Walker, E. A.; Nathan, D. M.; The Diabetes Prevention Program Research Group. Reduction in the incidence of type 2 diabetes with lifestyle intervention or metformin. *N. Engl. J. Med.* **2002**, *346*, 393−403.
(10) Hamman, R. F.; Wing, R. R.; Edelstein, S. L.; Lachin, J. M.; Bray, G. A.; Delahanty, L.; Hoskin, M.; Kriska, A. M.; Mayer-Davis, E. J.; Pi-Sunyer, X.; Regensteiner, J.; Venditti, B.; Wylie-Rosett, J. Effect of weight loss with lifestyle intervention on risk of diabetes. *Diabetes Care* **2006**, *29*, 2102−2107.
(11) Finelli, C.; Tarantino, G. Is visceral fat reduction necessary to favor metabolic changes in the liver? *J Gastrointestin Liver Dis* **2012**, *21*, 205−208.
(12) Muoio, D. M.; Newgard, C. B. Molecular and metabolic mechanisms of insulin resistance and β-cell failure in type 2 diabetes. *Nat. Rev. Mol. Cell Biol.* **2008**, *9*, 193−205.
(13) Cao, H. Adipocytokines in obesity and metabolic disease. *J. Endocrinol.* **2014**, *220*, T47−T59.
(14) Ruan, H.; Dong, L. Q. Adiponectin signaling and function in insulin target tissues. *J. Mol. Cell Biol.* **2016**, *8*, 101−109.
(15) Meyer, L. K.; Ciaraldi, T. P.; Henry, R. R.; Wittgrove, A. C.; Phillips, S. A. Adipose tissue depot and cell size dependency of adiponectin synthesis and secretion in human obesity. *Adipocyte* **2013**, *2*, 217−226.
(16) Okuno, A.; Tamemoto, H.; Tobe, K.; Ueki, K.; Mori, Y.; Iwamoto, K.; Umesono, K.; Akanuma, Y.; Fujiwara, T.; Horikoshi, H.; Yazaki, Y.; Kadowaki, T. Troglitazone increases the number of small adipocytes without the change of white adipose tissue mass in obese Zucker rats. *J. Clin. Invest.* **1998**, *101*, 1354−1361.
(17) Samuel, V. T.; Shulman, G. I. Integrating mechanisms for insulin resistance: Common threads and missing links. *Cell* **2012**, *148*, 852−871.
(18) Uemura, T.; Hirai, S.; Mizoguchi, N.; Goto, T.; Lee, J.-Y.; Taketani, K.; Nakano, Y.; Shono, J.; Hoshino, S.; Tsuge, N.; Narukami, T.; Takahashi, N.; Kawada, T. Diosgenin present in fenugreek improves glucose metabolism by promoting adipocyte differentiation and inhibiting inflammation in adipose tissues. *Mol. Nutr. Food Res.* **2010**, *54*, 1596−1608.
(19) Takahashi, S.; Waki, N.; Mohri, S.; Takahashi, H.; Ara, T.; Aizawa, K.; Suganuma, H.; Kawada, T.; Goto, T. Apo-12′-lycopenal, a lycopene metabolite, promotes adipocyte differentiation via peroxisome proliferator-activated receptor γ activation. *J. Agric. Food Chem.* **2018**, *66*, 13152−13161.
(20) Yamamoto, J.; Yamane, T.; Oishi, Y.; Shimizu, M.; Tadaishi, M.; Kobayashi-Hattori, K. Chrysanthemum promotes adipocyte differentiation, adiponectin secretion and glucose uptake. *Am. J. Chin. Med.* **2015**, *43*, 255−267.
(21) Yamamoto, J.; Tadaishi, M.; Yamane, T.; Oishi, Y.; Shimizu, M.; Kobayashi-Hattori, K. Hot water extracts of edible *Chrysanthemum morifolium* Ramat. exert antidiabetic effects in obese diabetic KK-A^{y} mice. *Biosci., Biotechnol., Biochem.* **2015**, *79*, 1147−1154.
(22) Harada, K.; Kato, Y.; Takahashi, J.; Imamura, H.; Nakamura, N.; Nishina, A.; Phay, N.; Tadaishi, M.; Shimizu, M.; Kobayashi-Hattori, K. The effect of methanolic Valeriana officinalis root extract on adipocyte differentiation and adiponectin production in 3T3-L1 adipocytes. *Plant Foods Hum. Nutr.* **2020**, *75*, 103−109.
(23) Orhan, I. E. A review focused on molecular mechanisms of anxiolytic effect of Valeriana officinalis L. in connection with its phytochemistry through in vitro/in vivo studies. *Curr. Pharm. Des.* **2021**, *27*, 3084−3090.
(24) Hendriks, H.; Bos, R.; Woerdenbag, H. J.; Koster, A. S. Central nervous depressant activity of valerenic acid in the mouse. *Planta Med.* **1985**, *51*, 28−31.
(25) Farmer, S. R. Transcriptional control of adipocyte formation. *Cell Metab.* **2006**, *4*, 263−273.
(26) Spranger, J.; Kroke, A.; Möhlig, M.; Bergmann, M. M.; Ristow, M.; Boeing, H.; Pfeiffer, A. F. Adiponectin and protection against type 2 diabetes mellitus. *Lancet* **2003**, *361*, 226−228.
(27) Ntambi, J. M.; Young-Cheul, Y.-C. Adipocyte differentiation and gene expression. *J. Nutr.* **2000**, *130*, 3122S−3126S.
(28) Nolte, R. T.; Wisely, G. B.; Westin, S.; Cobb, J. E.; Lambert, M. H.; Kurokawa, R.; Rosenfeld, M. G.; Willson, T. M.; Glass, C. K.; Milburn, M. V. Ligand binding and co-activator assembly of the peroxisome proliferator-activated receptor-γ. *Nature* **1998**, *395*, 137−143.
(29) Liberato, M. V.; Nascimento, A. S.; Ayers, S. D.; Lin, J. Z.; Cvoro, A.; Silveira, R. L.; Martínez, L.; Souza, P. C. T.; Saidemberg, D.; Deng, T.; Amato, A. A.; Togashi, M.; Hsueh, W. A.; Phillips, K.; Palma, M. S.; Neves, F. A. R.; Skaf, M. S.; Webb, P.; Polikarpov, I. Medium chain fatty acids are selective peroxisome proliferator activated receptor (PPAR) γ activators and pan-PPAR partial agonists. *PLoS One* **2012**, *7*, No. e36297.
(30) Wang, L.; Waltenberger, B.; Pferschy-Wenzig, E.-M.; Blunder, M.; Liu, X.; Malainer, C.; Blazevic, T.; Schwaiger, S.; Rollinger, J. M.; Heiss, E. H.; Schuster, D.; Kopp, B.; Bauer, R.; Stuppner, H.; Dirsch, V. M.; Atanasov, A. G. Natural product agonists of peroxisome proliferator-activated receptor gamma (PPARγ): A review. *Biochem. Pharmacol.* **2014**, *92*, 73−89.
(31) Kroker, A. J.; Bruning, J. B. Review of the structural and dynamic mechanism of PPARγ partial agonism. *PPAR Res.* **2015**, *2015*, 816856.
(32) Miyamae, Y. Insights into dynamic mechanism of ligand binding to peroxisome proliferator-activated receptor γ toward potential pharmacological applications. *Biol. Pharm. Bull.* **2021**, *44*, 1185−1195.
(33) Leesnitzer, L. M.; Parks, D. J.; Bledsoe, R. K.; Cobb, J. E.; Collins, J. L.; Consler, T. G.; Davis, R. G.; Hull-Ryde, E. A.; Lenhard, J. M.; Patel, L.; Plunket, K. D.; Shenk, J. L.; Stimmel, J. B.; Therapontos, C.; Willson, T. M.; Blanchard, S. G. Functional consequences of cysteine modification in the ligand binding sites of peroxisome proliferator activated receptors by GW9662. *Biochemistry* **2002**, *41*, 6640−6650.
(34) Waku, T.; Shiraki, T.; Oyama, T.; Maebara, K.; Nakamori, R.; Morikawa, K. The nuclear receptor PPARγ individually responds to serotonin- and fatty acid-metabolites. *EMBO J.* **2010**, *29*, 3395−3407.
(35) Park, H.-S.; Kim, S.-H.; Kim, Y. S.; Ryu, S. Y.; Hwang, J.-T.; Yang, H. J.; Kim, G.-H.; Kwon, D. Y.; Kim, M.-S. Luteolin inhibits adipogenic differentiation by regulating PPARgamma activation. *Biofactors* **2009**, *35*, 373−379.
(36) Ohtera, A.; Miyamae, Y.; Yoshida, K.; Maejima, K.; Akita, T.; Kakizuka, A.; Irie, K.; Masuda, S.; Kambe, T.; Nagao, M. Identification of a new type of covalent PPARγ agonist using a ligand-linking strategy. *ACS Chem. Biol.* **2015**, *10*, 2794−2804.
(37) Choi, J. H.; Banks, A. S.; Estall, J. L.; Kajimura, S.; Boström, P.; Laznik, D.; Ruas, J. L.; Chalmers, M. J.; Kamenecka, T. M.; Blüher, M.; Griffin, P. R.; Spiegelman, B. M. Obesity-linked phosphorylation of PPARγ by cdk5 is a direct target of the anti-diabetic PPARγ ligands. *Nature* **2010**, *466*, 451−456.
(38) Jang, J. Y.; Koh, M.; Bae, H.; An, D. R.; Im, H. N.; Kim, H. S.; Yoon, J. Y.; Yoon, H.-J.; Han, B. W.; Park, S. B.; Suh, S. W. Structural basis for differential activities of enantiomeric PPARγ agonists: Binding of S35 to the alternate site. *Biochim. Biophys. Acta Protein Proteonomics* **2017**, *1865*, 674−681.
(39) Anderson, G. D.; Elmer, G. W.; Taibi, D. M.; Vitiello, M. V.; Kantor, E.; Kalhorn, T. F.; Howald, W. N.; Barsness, S.; Landis, C. A. Pharmacokinetics of valerenic acid after single and multiple doses of valerian in older women. *Phytother Res.* **2010**, *24*, 1442−1446.
(40) Becker, A.; Felgentreff, F.; Schröder, H.; Meier, B.; Brattström, A. The anxiolytic effects of a Valerian extract is based on varelenic acid. *BMC Complementary Altern. Med.* **2014**, *14*, 267.
(41) Pan, X.; Wang, P.; Luo, J.; Wang, Z.; Song, Y.; Ye, J.; Hou, X. Adipogenic changes of hepatocytes in a high-fat diet-induced fatty liver mice model and non-alcoholic fatty liver disease patients. *Endocrine* **2015**, *48*, 834−847.

https://doi.org/10.1021/acsomega.2c06120
ACS Omega 2022, 7, 48113−48120

(42) Alkharfy, K. M.; Frye, R. F. Effect of valerian, valerian/hops extracts, and valerenic acid on glucuronidation in vitro. *Xenobiotica* **2007**, *37*, 113−123.
(43) Maier-Salamon, A.; Trauner, G.; Hiltscher, R.; Reznicek, G.; Kopp, B.; Thalhammer, T.; Jäger, W. Hepatic metabolism and biliary excretion of valerenic acid in isolated perfused rat livers: role of Mrp2 (Abcc2). *J. Pharm. Sci.* **2009**, *98*, 3839−3849.
(44) Kara, M.; Öztaş, E.; Boran, T.; Karaman, E. F.; Veskoukis, A. S.; Tsatsakis, A. M. Ameliorative effects of the sesquiterpenoid valerenic acid on oxidative stress induced in HepG2 cells after exposure to the fungicide benomyl. *Antioxidants* **2021**, *10*, 746.
(45) Senarath, S.; Beppu, F.; Yoshinaga, K.; Nagai, T.; Yoshida, A.; Gotoh, N. Comparison of the effects of long-chain monounsaturated fatty acid positional isomers on lipid metabolism in 3T3-L1 cells. *J. Oleo Sci.* **2019**, *68*, 379−387.
(46) Manaharan, T.; Ming, C. H.; Palanisamy, U. D. Syzygium queum leaf extract and its bioactive compounds enhances pre-adipocyte differentiation and 2-NBDG uptake in 3T3-L1 cells. *Food Chem.* **2013**, *136*, 354−363.
(47) Sakamoto, T.; Takahashi, N.; Sawaragi, Y.; Naknukool, S.; Yu, R.; Goto, T.; Kawada, T. Inflammation induced by RAW macrophages suppresses UCP1 mRNA induction via ERK activation in 10T1/2 adipocytes. *Am. J. Physiol. Cell Physiol.* **2013**, *304*, C729−C738.
(48) Takahashi, N.; Kawada, T.; Goto, T.; Yamamoto, T.; Taimatsu, A.; Matsui, N.; Kimura, K.; Saito, M.; Hosokawa, M.; Miyashita, K.; Fushiki, T. Dual action of isoprenols from herbal medicines on both PPARγ and PPARα in 3T3-L1 adipocytes and HepG2 hepatocytes. *FEBS Lett.* **2002**, *514*, 315−322.

https://doi.org/10.1021/acsomega.2c06120
ACS Omega 2022, 7, 48113−48120